Thermodynamic Properties of Alkali Nitrate–Silver Nitrate Melts

J. RICHTER and S. SEHM

Lehrstuhl für Physikalische Chemie II der Rheinisch-Westfälischen Technischen Hochschule Aachen

(Z. Naturforsch. **27 a**, 141—148 [1972]; received 5 October 1971)

EMF measurements were performed on a chemical cell containing a silver and a nitrate electrode. The systems $NaNO_3+AgNO_3$, $LiNO_3+AgNO_3$, and pure $AgNO_3$ were investigated in a temperature range of 240 °C to 310 °C and in the total concentration range permitted by the phase diagram. We found a linear dependence of the EMF on temperature. Six constants, characteristic for the investigated molten salts depending neither on composition nor on temperature, were determined by the analytical construction of the activity coefficients. Together with the analytically constructed excess molar Gibbs function, the excess molar entropy was calculated from calorimetric data in the literature.

There are two different possibilities for the determination of the activity coefficients in molten salts: vapour pressure measurements and EMF measurements on chemical cells. The method of vapour pressure measurements is uncertain; it has been shown by mass spectrometric investigations [1–5] that a number of sequesterings and associations may be present in the vapour phase of molten salts, which complicates or prevents the analysis of the vapour pressure data.

The purpose of this paper is to determine the activity coefficients and other thermodynamic functions of the systems $NaNO_3+AgNO_3$ and $LiNO_3+AgNO_3$ as functions of composition and temperature. This will be achieved by EMF measurements on the chemical cells

$$\mathrm{Cu}\,|\,\mathrm{Ag}\,|\,\mathrm{NaNO_3+AgNO_3}\,|\,\mathrm{O_2, NO_2(Pt)}\,|\,\mathrm{Cu} \quad (1)$$

and

$$\mathrm{Cu}\,|\,\mathrm{Ag}\,|\,\mathrm{LiNO_3+AgNO_3}\,|\,\mathrm{O_2, NO_2(Pt)}\,|\,\mathrm{Cu}, \quad (2)$$

respectively.

The symbol $O_2, NO_2(Pt)$ indicates a nitrate electrode with a platinum matrix developed by KETELAAR and DAMMERS-DEKLERK [6, 7]. Ag symbolizes a silver electrode and Cu the copper terminals of the cell.

Basic Equations

Activity coefficients for molten salts describe the deviation from the standardized ideal mixture. The standardized ideal mixture is characterized by the condition that total dissociation exists in the melt which is an ideal mixture with respect to the individual species, and that no complex ions are found.

The activity coefficients are defined [8–11] by the equation

$$\ln f_i \equiv \psi_i - \psi_i^{\mathrm{id}} \quad (i=1,2). \quad (3)$$

The activity coefficient f_i of the component i is dimensionless and a function of the thermodynamic temperature T, of the pressure P, and of the mole fraction $x \equiv x_2$ of component 2. The limiting values of the activity coefficients of the pure liquid components are 1 as are those of nonelectrolyte solutions.

ψ_i is the dimensionless quantity

$$\psi_i \equiv (\mu_i - \mu_i^{\cdot})/RT. \quad (4)$$

Here R denotes the gas constant, μ_i the chemical potential of the component i in the melt and $\mu_i^{\cdot}$ the chemical potential of the pure liquid component i at the given values of T and P. ψ_i^{id} is the value of ψ_i for a standardized ideal melt of the same composition.

From Eqs. (3) and (4) we obtain for the excess chemical potential

$$\mu_i^{\mathrm{E}} \equiv \mu_i - \mu_i^{\mathrm{id}} = RT \ln f_i \quad (5)$$

where μ_i^{id} is the value of μ_i for a standardized ideal melt.

For cells (1) and (2) we have

$$F\Phi = A \quad (6)$$

where F is the Faraday constant, Φ the EMF and A the affinity of the reaction

$$\underset{(\mathrm{solid})}{\mathrm{Ag}} + \underset{(\mathrm{gaseous})}{\mathrm{NO_3}} + \underset{(\mathrm{gaseous})}{\tfrac{1}{2}\,\mathrm{O_2}} \rightarrow \underset{(\mathrm{liquid})}{\mathrm{AgNO_3}}. \quad (7)$$

Reprint requests to Dr. J. RICHTER, Lehrstuhl für Physikal. Chemie II der Rhein.-Westf. Technischen Hochschule, *D-5100 Aachen*, Templergraben 59.

If we denote the EMF of the cell

$$\mathrm{Cu}\,|\,\mathrm{Ag}\,|\,\mathrm{AgNO_3}\,|\,\mathrm{O_2},\mathrm{NO_2(Pt)}\,|\,\mathrm{Cu} \qquad (8)$$

by $\Phi^{\cdot}$ and the affinity of the heterogeneous reaction belonging to (8) by $A^{\cdot}$ we find with Eq. (6):

$$F(\Phi-\Phi^{\cdot})=A-A^{\cdot}. \qquad (9)$$

For reaction (7), we have explicitely:

$$A=\mu_{\mathrm{Ag}}+\mu_{\mathrm{NO_2}}+\tfrac{1}{2}\,\mu_{\mathrm{O_2}}-\mu_2\,, \qquad (10)$$

$$A^{\cdot}=\mu_{\mathrm{Ag}}+\mu_{\mathrm{NO_2}}+\tfrac{1}{2}\,\mu_{\mathrm{O_2}}-\mu_2^{\cdot}, \qquad (11)$$

where μ_{Ag} denotes the chemical potential of solid silver, $\mu_{\mathrm{NO_2}}$ the chemical potential of gaseous nitrogen dioxide, $\mu_{\mathrm{O_2}}$ the chemical potential of gaseous oxygen and μ_2 and $\mu_2^{\cdot}$ the chemical potentials of liquid silver nitrate in the melt and in the pure state, respectively.

Since for a given temperature and total pressure, the partial vapour pressures of nitrogen dioxide and oxygen are constant, it follows from Eq. (9) with (10) and (11) that

$$F(\Phi-\Phi^{\cdot})=\mu_2^{\cdot}-\mu_2\,. \qquad (12)$$

For the activity coefficients f_2 of the silver nitrate in the binary melts $\mathrm{NaNO_3}+\mathrm{AgNO_3}$ and $\mathrm{LiNO_3}+\mathrm{AgNO_3}$, taking account of Eqs. (3), (4), (12), and the relations

$$\psi_i^{\mathrm{id}}=\ln(1-x), \quad \psi_2^{\mathrm{id}}=\ln x\,, \qquad (13)$$

valid for molten salts containing two uni-univalent electrolytes with a common ion[10], we obtain the equation

$$\ln f_2=\frac{F(\Phi^{\cdot}-\Phi)}{RT}-\ln x\,. \qquad (14)$$

The experiments will be evaluated by means of this formula.

The excess molar Gibbs function $\overline{G}^{\mathrm{E}}$ for binary molten salts is given by

$$\overline{G}^{\mathrm{E}}=x(1-x)\,(a'+b'\,x+c'\,x^2), \qquad (15)$$

where only three terms have been retained. Thus we derive the following series expansions for the activity coefficients[12]:

$$\mu_1^{\mathrm{E}}=RT\ln f_1=A_2\,x^2+A_3\,x^3+A_4\,x^4+\ldots, \qquad (16)$$

$$\mu_2^{\mathrm{E}}=RT\ln f_2=B_2(1-x)^2+B_3(1-x)^3+B_4(1-x)^4+\ldots\,. \qquad (17)$$

The coefficients in Eqs. (15) to (17) still depend on T and P. If we truncate the power series after the third term, we find:

$$A_2=a'-b', \quad A_3=2(b'-c'), \quad A_4=3\,c', \qquad (18)$$

$$B_2=a'+2\,b'+3\,c', \quad B_3=-2(b'+3\,c'), \quad B_4=3\,c'. \qquad (19)$$

By differentiation with respect to T, we theoretically get the excess molar entropy $\overline{S}^{\mathrm{E}}$ and the molar heat of mixing $\overline{H}^{\mathrm{E}}$ from the temperature dependence of $\overline{G}^{\mathrm{E}}$. This procedure seldom leads to satisfactory results. This is even true for very precise vapour pressure measurements on aqueous elecrolyte solutions and on binary nonelectrolyte solutions. The reason for this is that differentiation of measured values with respect to one of the variables is too sensitive a test for experimental accuracy. Thus we prefer to compute the excess molar entropy $\overline{S}^{\mathrm{E}}$ from $\overline{G}^{\mathrm{E}}$ and $\overline{H}^{\mathrm{E}}$:

$$\overline{S}^{\mathrm{E}}=\frac{\overline{H}^{\mathrm{E}}-\overline{G}^{\mathrm{E}}}{T}\,. \qquad (20)$$

This is a better procedure to obtain $\overline{S}^{\mathrm{E}}$.

Experimental

For the preparation of the binary melts the following chemicals were used: Sodium nitrate (pro analysi) from E. Merck (Darmstadt), lithium nitrate (pro analysi) from Riedel-de Haën (Hannover), and silver nitrate, double recrystallized (Sonderqualität A) from Degussa (Frankfurt-M.).

The NO_2, O_2 gas mixture was prepared with purified oxygen from Linde (Köln) and liquid nitrogen tetroxide (purum) from Fluka (Buchs, Switzerland).

Water remaining in the salts influences the results. Therefore, the salts were dried carefully.

The type of apparatus used corresponds to that described by KETELAAR and DAMMERS-DEKLERK[6, 7]. We should like to draw attention to the following points important for our experiments:

1. An exact control and measurement of temperature is necessary since the temperature dependence of the EMF is very pronounced. Temperature profiles within the cell are to be avoided.
2. For the silver electrode, there should be no phase boundary between the protective gas and the molten salt, and there should be no recrystallization.
3. The NO_2, O_2 (Pt) electrode should work reversibly for a long time and without capillary effects The NO_2, O_2 gas mixture has to be replaced continuously so that a constant composition of the gases is given at the nitrate electrode.
4. The decomposition of the silver nitrate has to be avoided by performing the measurements only up to 310 °C and by protecting the melt with an inert gas atmosphere.

The cell and the electrodes are represented together with the furnace in Figure 1. The cell consists of a U-shaped glass tube (Duran 50 of Schott, Mainz), into which the nitrate electrode is introduced and the silver electrode and thermocouple are fixed. The cell

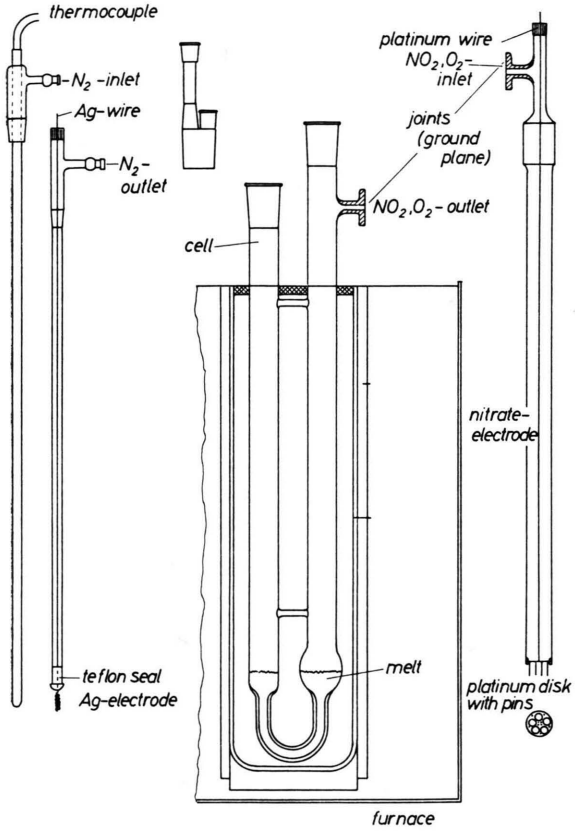

Fig. 1. Assembly of the cell, the electrodes, and the furnace.

is connected to the NO_2, O_2 gas mixture circulation by special joints which were ground plane. The arrangement was located in a standing tube furnace of Titan (Klarenthal-Saar), which was controlled by a transistor-inductive-controller with one-sided, thermal feedback.

The nitrate electrode differs in its assembly from that described by KETELAAR and DAMMERS-DEKLERK [6]. It consists of a platinum disk with a glass tube, which serves as the supply line for the NO_2, O_2 gas mixture (Fig. 1). From the platinum disk fused into the glass tube, a platinum wire leads upwards and goes outwards trhough a teflon-paraffin seal. At the lower side of the disk are 10 platinum pins, which are 10 mm long and 0,2 mm thick. They are welded on the disk at regular intervals. The platinum disk is 15 mm in diameter and has five boreholes (ϕ 4 mm), through which the NO_2, O_2 mixture can stream just along the platinum pins without any pressure rise. The pins plunge 3 to 4 mm into the melt. The atmosphere above the melt, into which the nitrate electrode plunges, is flushed away by the NO_2, O_2 mixture.

The mixture of oxygen and nitrogen dioxide is produced by slowly bubbling oxygen through a wash bottle filled with liquid nitrogen tetroxide. The procedure is represented in Figure 2. The oxygen is passed into the N_2O_4-saturator, kept at 18 °C by a thermostat. The gas mixture leaving the saturator consists of oxy-

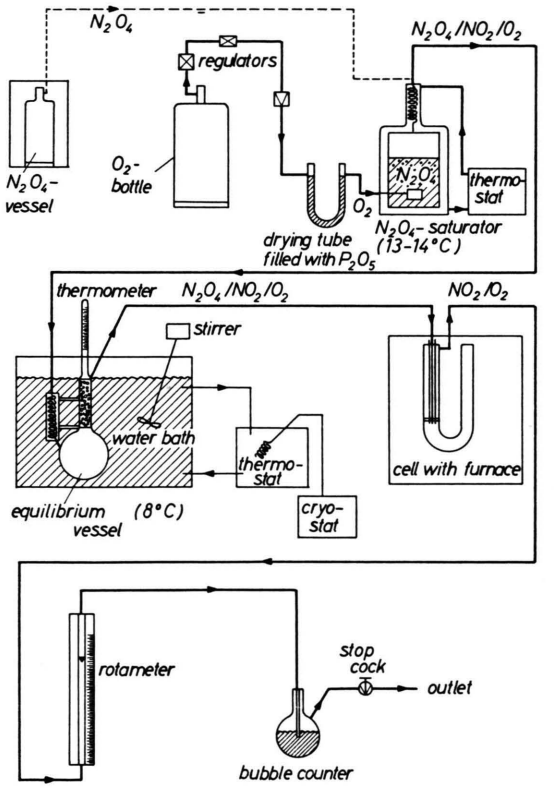

Fig. 2. Procedure for the production of the NO_2, O_2 gas mixture.

gen, nitrogen dioxide, and nitrogen tetroxide. It is led over a drying tube filled with phosphorus pentoxide to the equilibrium vessel kept at 8 °C by a thermostat.

The composition of the resulting gas mixture can be calculated from the vapour pressure of the liquid nitrogen tetroxide, its degree of dissociation at 8 °C, and from the total pressure (atmospheric pressure). Corresponding values are tabulated by GIAUQUE and KEMP [13]. As the remaining nitrogen tetroxide is completely dissociated into nitrogen dioxide at 250 °C to 300 °C, only nitrogen dioxide and oxygen appear at the electrode — an equimolar mixture for the above conditions. KETELAAR and DAMMERS-DEKLERK [6] find optimum EMF values for pure silver nitrate with an equimolar gas mixture. We find with Eqs. (10), (11), and (14) that the gas composition does not influence the values of the activity coefficients.

The gas mixture is led from the cell through a rotameter serving as flowmeter to a bubble counter and then through a stopcock to the outlet. The bubble counter contains phthalic acid-dibutylester which serves to isolate the gas system from the atmosphere.

Temperature measurement of the melt was performed directly at the silver electrode with a copper-constantan-thermocouple calibrated with mercury thermometers. The potential difference at the electrodes and the thermopotential of the thermocouple were monitored by two continuously working, automatically recording compensation recorders and measured by a cascade compensator of Feussner in the usual compensation circuit [14].

Results

The EMF (Φ) is measured as a function of composition and temperature. The lower limit of the temperature range in the system $NaNO_3 + AgNO_3$ is given by the phase diagram [15] which indicates that measurements in the composition range $x \leqq 0.4$ (x is the mole fraction of $AgNO_3$) are possible only above 280 °C. The temperature of 240 °C can be chosen as the lower limit for the entire concentration range for the system $LiNO_3 + AgNO_3$, in view of the phase diagram [16].

We find a linear dependence of the EMF on temperature in the investigated range of composition and temperature, within experimental accuracy. This temperature dependence can be represented by

$$\Phi = a + b\,(T - 273.15\,\mathrm{K}). \qquad (21)$$

The coefficients a and b depend on the mole fraction x. The straight lines corresponding to Eq. (21) are plotted in Fig. 3 for the system $NaNO_3 + AgNO_3$ and in Fig. 4 for the system $LiNO_3 + AgNO_3$.

The activity coefficients f_2 of silver nitrate calculated from the EMF (Φ) according to Eq. (14) are given in Table 1 for the system $NaNO_3 + AgNO_3$ as a function of composition at several temperatures. Table 2 contains the corresponding values for the system $LiNO_3 + AgNO_3$.

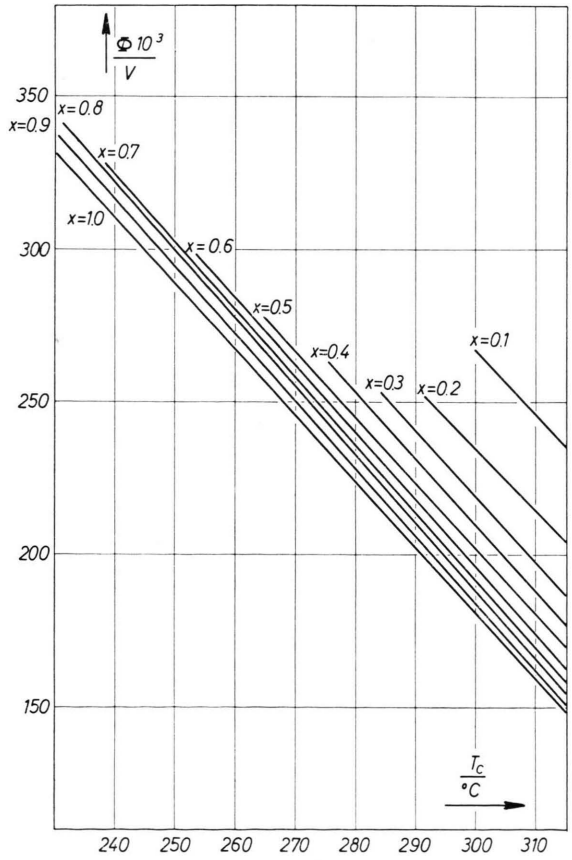

Fig. 3. $NaNO_3 + AgNO_3$: EMF (Φ) as a function of temperature T_C with the mole fraction x of silver nitrate as a parameter.

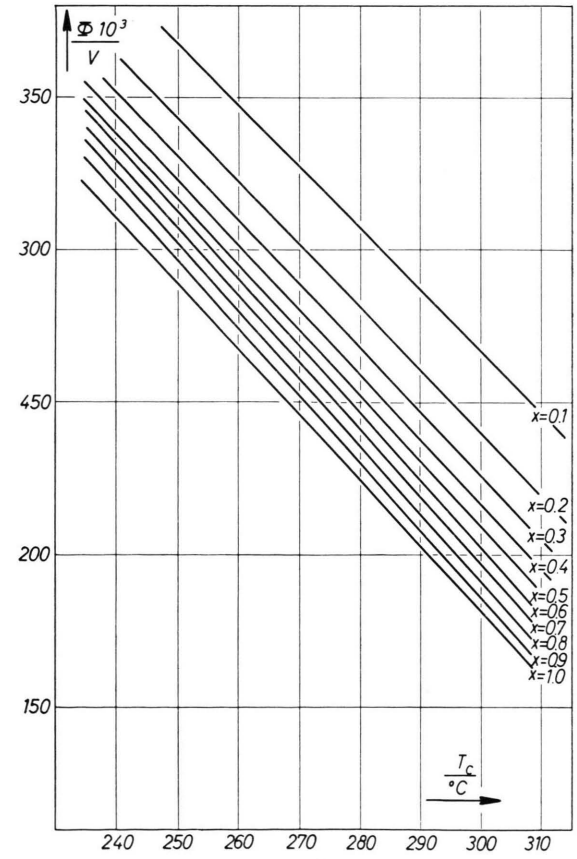

Fig. 4. $LiNO_3 + AgNO_3$: EMF (Φ) as a function of temperature T_C with the mole fraction x of silver nitrate as a parameter.

Table 1. $NaNO_3+AgNO_3$: Activity coefficients as a function of the mole fraction x of silver nitrate at different temperatures.

x	240 °C	250 °C	260 °C	270 °C	280 °C	290 °C	300 °C	310 °C
0.95	0.980	0.982	0.997	1.001	1.006	1.014	1.016	1.020
0.90	0.975	0.975	0.994	1.005	1.016	1.030	1.035	1.044
0.85	0.970	0.979	0.997	1.016	1.031	1.042	1.060	1.071
0.80	0.973	0.994	1.007	1.033	1.053	1.070	1.089	1.099
0.70	1.011	1.051	1.064	1.088	1.111	1.130	1.149	1.168
0.65		1.093	1.112	1.130	1.149	1.172	1.183	1.204
0.60		1.145	1.160	1.176	1.190	1.212	1.222	1.243
0.50				1.270	1.272	1.294	1.308	1.322
0.40					1.380	1.390	1.412	1.410
0.30						1.533	1.533	1.524
0.20							1.676	1.661
0.15							1.843	1.737
0.10								1.818

Table 2. $LiNO_3+AgNO_3$: Activity coefficients as a function of the mole fraction x of silver nitrate at different temperatures.

x	240 °C	250 °C	260 °C	270 °C	280 °C	290 °C	300 °C	310 °C
0.90	0.929	0.950	0.967	0.975	0.988	1.003	1.008	1.015
0.80	0.910	0.932	0.953	0.970	0.990	1.013	1.022	1.036
0.85	0.912	0.937	0.954	0.975	0.998	1.022	1.032	1.048
0.70	0.922	0.948	0.962	0.988	1.008	1.032	1.045	1.061
0.60	0.970	0.996	1.007	1.030	1.046	1.062	1.077	1.111
0.55	1.006	1.032	1.042	1.063	1.074	1.086	1.101	1.125
0.50	1.055	1.075	1.085	1.098	1.109	1.120	1.131	1.153
0.45	1.112	1.124	1.135	1.146	1.154	1.167	1.170	1.188
0.40	1.174	1.182	1.191	1.201	1.210	1.220	1.220	1.230
0.35	1.241	1.248	1.260	1.263	1.275	1.285	1.285	1.286
0.30	1.316	1.325	1.334	1.338	1.348	1.353	1.361	1.360
0.25	1.406	1.407	1.421	1.423	1.426	1.428	1.441	1.445
0.20	1.505	1.506	1.512	1.514	1.515	1.522	1.529	1.537
0.15	1.602	1.614	1.615	1.616	1.624	1.635	1.634	1.652
0.10		1.736	1.740	1.745	1.754	1.767	1.771	1.776

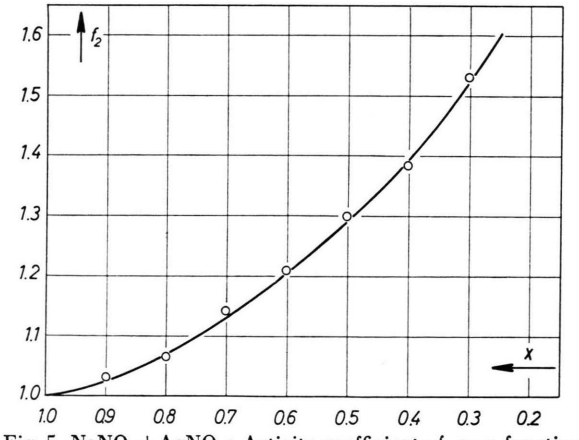

Fig. 5. $NaNO_3+AgNO_3$: Activity coefficients f_2 as a function of the mole fraction x of silver nitrate at $T_c=290$ °C.

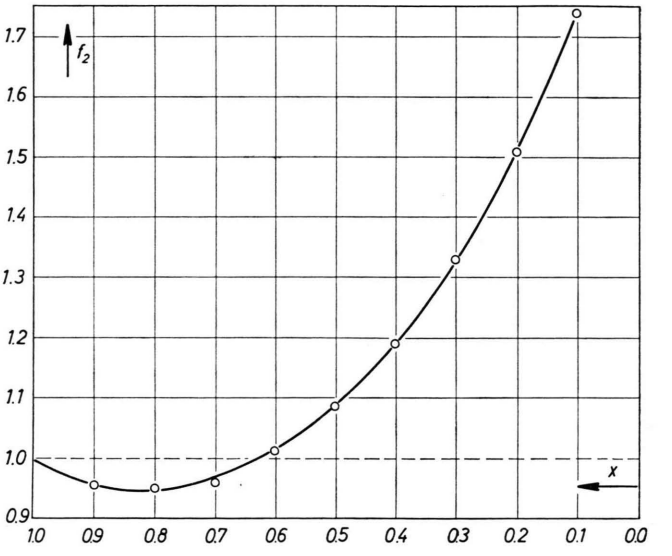

Fig. 6. $LiNO_3+AgNO_3$: Activity coefficients f_2 as a function of the mole fraction x of silver nitrate at $T_c=260$ °C. →

In Fig. 5 the activity coefficient f_2 of silver nitrate for the system $LiNO_3 + AgNO_3$ is plotted against mole fraction at 290 °C. Figure 6 shows f_2 for the system $LiNO_3 + AgNO_3$ vs. x at 260 °C.

We see that f_2 always remains greater than 1 above 270 °C in the $NaNO_3 + AgNO_3$ system and above 290 °C in the $LiNO_3 + AgNO_3$ system. Below these temperatures, the activity coefficients of the melts rich in silver nitrate are less than 1.

Discussion

From the linear temperature dependence of the EMF [Eq. (21)] at constant composition, we derive for the logarithm of the activity coefficients:

$$R \ln f_2 = A/T + B . \qquad (22)$$

The coefficients A and B depend only on composition.

The logarithms of the activity coefficients are represented by the series expansions (16) and (17) with integral powers. We see that the power series can be truncated after the third term for the two systems investigated here. The concentration dependence of the activity coefficients is thus adequately described within experimental accuracy.

The coefficients B_2, B_3, and B_4 in Eq. (17) depend only on temperature, since the pressure is kept constant. Since, on the other hand, the logarithms of the activity coefficients at constant composition depend linearly on the reciprocal temperature, according to Eq. (22), the coefficients B_2, B_3, and B_4 must be linear in T. Thus we obtain:

$$B_2 = \alpha_0 + \beta_0 T , \qquad (23)$$

$$B_3 = \alpha_1 + \beta_1 T , \qquad (24)$$

$$B_4 = \alpha_2 + \beta_2 T . \qquad (25)$$

The constants α_0, β_0, α_1, β_1, and α_2, β_2 are characteristic for each pair of molten salts and independent of composition and temperature. With these constants we can, in principle, compute all the thermodynamic quantities at any composition and temperature.

We can determine these constants α_0, β_0, α_1, β_1, and α_2, β_2 from the temperature dependence of the coefficients B_2, B_3, and B_4 of Eq. (17). For different temperatures the coefficients B_2, B_3, and B_4 are determined so that they describe adequately the concentration slope of the activity coefficients within experimental accuracy except in the limiting range. (In the limiting range $x \to 1$, the relative error of the measured difference $\Phi' - \Phi$ [Eq. (14)] is greater than the experimental accuracy in the remaining concentration range. For this reason the limiting behavior of the activity coefficients cannot be investigated experimentally by the method developed here.)

From the graphical plots of the coefficients B_2, B_3, and B_4, we can determine the constants α_0, β_0, α_1, β_1, and α_2, β_2 by the equations of the straight lines (23) to (25). The coefficients B_2, B_3, and B_4 thus obtained are given in Table 3 as functions of temperature; the constants α_0, β_0, α_1, β_1, and α_2, β_2 are shown in Table 4.

Table 3. Coefficients B_2, B_3, and B_4 of the analytical representation of the activity coefficients for the systems $NaNO_3 + AgNO_3$ and $LiNO_3 + AgNO_3$.

T_c / °C	$B_2 \cdot 10^{-3}$ / J mol^{-1}	$B_3 \cdot 10^{-3}$ / J mol^{-1}	$B_4 \cdot 10^{-3}$ / J mol^{-1}
$NaNO_3 + AgNO_3$			
260	− 2.47	18.62	− 10.46
270	1.09	9.62	− 5.52
280	4.60	0.25	− 0.67
290	8.57	− 9.16	3.68
300	12.22	− 18.03	9.25
310	15.86	− 27.24	14.73
$LiNO_3 + AgNO_3$			
240	− 9.96	31.97	− 20.29
250	− 8.12	27.28	− 16.95
260	− 6.32	22.43	− 13.60
270	− 4.48	17.53	− 10.29
280	− 2.64	12.68	− 7.20
290	− 0.75	7.82	− 3.81
300	1.09	3.01	− 0.67
310	3.05	1.84	2.59

Table 4. Characteristic constants α_0, β_0, α_1, β_1, and α_2, β_2 for the systems $NaNO_3 + AgNO_3$ and $LiNO_3 + AgNO_3$.

$NaNO_3 + AgNO_3$	
α_0 =	− 196.600 · 10^3 J mol^{-1}
β_0 =	0.364 · 10^3 J mol^{-1} K^{-1}
α_1 =	501.700 · 10^3 J mol^{-1}
β_1 =	− 0.907 · 10^3 J mol^{-1} K^{-1}
α_2 =	− 275.700 · 10^3 J mol^{-1}
β_2 =	0.497 · 10^3 J mol^{-1} K^{-1}
$LiNO_3 + AgNO_3$	
α_0 =	− 103.800 · 10^3 J mol^{-1}
β_0 =	0.183 · 10^3 J mol^{-1} K^{-1}
α_1 =	279.900 · 10^3 J mol^{-1}
β_1 =	− 0.483 · 10^3 J mol^{-1} K^{-1}
α_2 =	− 187.800 · 10^3 J mol^{-1}
β_2 =	0.327 · 10^3 J mol^{-1} K^{-1}

The coefficients a', b', and c' of the analytical form (15) of the excess molar Gibbs function can be calculated by Eq. (19) from the experimentally investigated coefficients B_2, B_3, and B_4; a', b', and c' for the systems $NaNO_3 + AgNO_3$ and $LiNO_3 + AgNO_3$ are summarized in Table 5.

Table 5. Coefficients a', b', and c' of the analytical representation of the molar excess function $\bar{G}^E$ for the systems $NaNO_3+AgNO_3$ and $LiNO_3+AgNO_3$.

T_c / °C	$a' \cdot 10^{-3}$ / J mol^{-1}	$b' \cdot 10^{-3}$ / J mol^{-1}	$c' \cdot 10^{-3}$ / J mol^{-1}
$NaNO_3 + AgNO_3$			
260	5.69	1.15	− 3.49
270	5.19	0.71	− 1.84
280	4.18	0.54	− 0.22
290	3.10	0.90	1.13
300	3.43	− 0.23	3.08
310	3.34	− 1.11	4.91
$LiNO_3 + AgNO_3$			
240	1.72	4.31	− 6.76
250	2.22	3.31	− 5.65
260	2.51	2.39	− 4.53
270	2.76	1.52	− 3.43
280	2.85	0.86	− 2.40
290	3.26	− 0.10	− 1.27
300	3.43	− 0.84	− 0.22
310	3.81	− 1.68	− 0.85

By means of the calorimetric data for the molar heat of mixing of the two systems, measured by KLEPPA and coworkers [17], we can compute the excess molar entropy by Eqs. (15) and (20). In Fig. 7 the thermodynamic functions for the system $NaNO_3 + AgNO_3$ at 290 °C are plotted, and in Fig. 8 those for the system $LiNO_3 + AgNO_3$ at 260 °C.

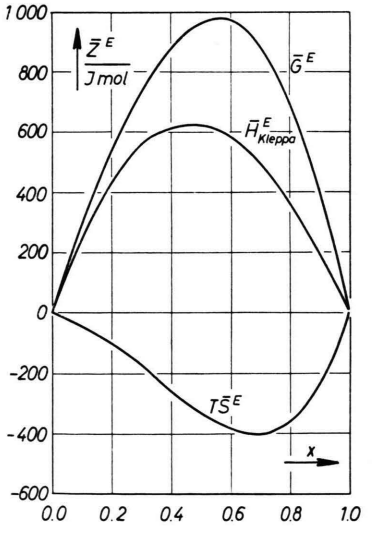

Fig. 7. $NaNO_3+AgNO_3$: Molar excess functions $\bar{G}^E$, $\bar{H}^E$, and $T\,S^E$ as functions of the mole fraction x of silver nitrate at $T_c=290$ °C.

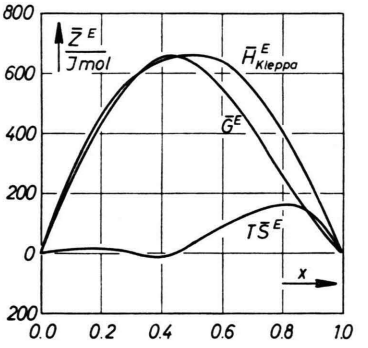

Fig. 8. $LiNO_3+AgNO_3$: Molar excess functions $\bar{G}^E$, $\bar{H}^E$, and $T\,S^E$ as functions of the mole fraction x of silver nitrate at $T_c=260$ °C.

If we take the equation of the partial molar enthalpy of mixing [18]

$$\bar{H}_2^E = \mu_2^E - T(\partial \mu_2^E/\partial T)_x, \qquad (26)$$

we find with Eqs. (5) and (26) that

$$\bar{H}_2^E = R(\partial \ln f_2/\partial\, 1/T)_x. \qquad (27)$$

At constant mole fraction x, it follows from Eq. (27) with (22) that

$$\bar{H}_2^E = A = \text{const}. \qquad (28)$$

Equation (28) means that $\bar{H}^E$ is independent of the temperature for both systems investigated here. Thus it has been shown that the values of $\bar{H}^E$ measured by KLEPPA and coworkers [17] at 350 °C can be consistently combined with the measurements performed here.

In the system $NaNO_3 + AgNO_3$ the values of $\bar{G}^E$ are remarkably greater than the values of $\bar{H}^E$; in the system $LiNO_3 + AgNO_3$ they are of the same order. Therefore we might describe the system $LiNO_3 + AgNO_3$, to the first approximation, as a "regular mixture", defined by the conditions

$$\bar{G}^E = \bar{H}^E, \quad \bar{S}^E = 0\ [18].$$

The "symmetry rule of HAASE" [12] holds for both systems: the excess molar Gibbs function is nearly symmetrical, while the other functions, in particular $\bar{S}^E$, deviate considerably from the symmetrical form.

Conclusions

Inserting Eq. (23) – (25) into (17) we obtain

$$RT \ln f_2 = (\alpha_0 + \beta_0 T)(1-x)^2 + (\alpha_1 + \beta_1 T)(1-x)^3 + (\alpha_2 + \beta_2 T)(1-x)^4. \quad (29)$$

For a certain temperature T with the mole fraction $(1-x)$ as parameter, a system of six linear equations can be derived from Eq. (29), together with the well-known activity coefficients. These equations may serve to determine the six constants. If this procedure is carried out for different temperatures and for any value of the mole fraction, one obtains different values of the constants, which no longer rigorously describe the determined concentration slope of the activity coefficients. Therefore, the procedure used above is better: the computation of the constants from the temperature dependence of the coefficients B_2, B_3, and B_4.

Using the constants α_0, β_0, α_1, β_1, and α_2, β_2 we may compute all the thermodynamic functions, in principle. The accuracy of this direct calculation is lower than the possible experimental accuracy, in view of the differential connection of the thermodynamic quantities. Therefore, the EMF measurements are best combined with calorimetric data for the calculation of the thermodynamic functions.

Acknowledgment

We are obliged to Prof. Dr. R. HAASE for many discussions and helpful advice. – This investigation was supported by the Deutsche Forschungsgemeinschaft.

[1] R. F. PORTER and R. C. SCHOONMAKER, J. Chem. Phys. **29**, 1074 [1958].
[2] J. BERKOWITZ and W. A. CHUPKA, Ann. N. Y. Acad. Sci. **79**, 1073 [1960].
[3] E. E. SCHRIER and H. M. CLARK, J. Phys. Chem. **67**, 1259 [1963].
[4] M. BLANDER, J. Chem. Phys. **41**, 170 [1964].
[5] H. BLOOM and J. W. HASTIE, J. Phys. Chem. **72**, 2706 [1968].
[6] J. A. A. KETELAAR and A. DAMMERS-DEKLERK, Rec. Trav. Chim. **83**, 322 [1964].
[7] J. A. A. KETELAAR and A. DAMMERS-DEKLERK, Proc. Nederl. Ak. **68**, B, 169 [1965].
[8] R. HAASE, Z. Phys. Chem. Frankfurt **63**, 95 [1969].
[9] R. HAASE, J. Phys. Chem. **73**, 1160 [1969].
[10] J. RICHTER, Z. Naturforsch. **24 a**, 447 [1969].
[11] R. HAASE, Z. Naturforsch. **26 a**, 783 [1971].
[12] J. RICHTER, Z. Naturforsch. **24 a**, 835 [1969].
[13] W. F. GIAUQUE and J. D. KEMP, J. Chem. Phys. **6**, 40 [1938].
[14] For more details of the experimental section see: S. SEHM, Thesis, Aachen 1971.
[15] D. J. HISSINK, Z. Phys. Chem. **32**, 537 [1900].
[16] C. SINISTRI and P. FRANZOSINI, Ric. Sci. **33** (II-A), 419 [1963].
[17] O. J. KLEPPA, R. B. CLARKE, and L. S. HERSH, J. Chem. Phys. **35**, 175 [1961].
[18] R. HAASE, Thermodynamik der Mischphasen, Springer-Verlag, Berlin 1956.